SurfSeis 4

User's Manual

Table of Contents

Introduction

The purpose of this manual is to highlight the new features in SurfSeis 4.0. This manual is intended to be used in conjunction with the manuals from previous versions of SurfSeis (1.5, 2.05, and 3.0). All the manual files are in the "Manual" subfolder of the SurfSeis 4 application folder (e.g., C:\SurfSeis4\Manual). This SurfSeis 4 supplementary user's manual (short version) provides the essential information necessary for our users to operate this newest version of our software.

The multichannel analysis of surface waves (MASW) method has been under development since the mid-1990s at the Kansas Geological Survey (KGS). Each new version of our software includes components that reflect our most recent research. The following are the most significant new features in SurfSeis 4:

1. Sliding window passive data dispersion-curve imaging
2. Flexible input of a-priori initial-model parameters, such as compressional velocity (Vp), Poisson's ratio, and density.
3. Ongoing-inversion 2-D monitoring
4. High-Resolution Linear Radon Transform (HRLRT) for dispersion-curve imaging (optional, included in SurfSeis 4.2)
5. Licensing now compatible with Windows 8

This manual has three main sections, each reflecting developments in SurfSeis software. The first section addresses the most recent research—sliding window passive signal analysis. The second section presents a new 2-D imaging tool that incorporates 2-D a-priori information into the initial model(s) to facilitate the dispersion-curve inversion. Initial shear-wave velocity (Vs), compressional-wave velocity (Vp) or Poisson's ratio (PR), and density can now be incorporated in any of a variety of combinations. The third section introduces the new HRLRT complete with data examples and synthetic data as seen in several publications (Luo et al., 2008; Ivanov et al., 2010; Zeng et al., 2012; Pan et al., 2013).

Our users have suggested other minor improvements, which we have made. A primary goal of SurfSeis 4 is to enrich a-priori information data input. We hope that we've succeeded, but we also realize that although we always test many possibilities, there are likely some functionality issues that can be tuned up or improved. We rely on our users for feedback and suggestions and we, the KGS staff, sincerely appreciate your comments and help in improving the SurfSeis software.

Sliding window passive data dispersion-curve imaging

The sliding window passive-data dispersion-curve imaging algorithm was developed for better imaging by taking advantage of multiple and variable passive sources active during the recording time. It was originally developed for a site where distant trains were used as multiple passive sources (Ivanov et al., 2013). The data example used in the manuscript was 32 s long. In comparison to the conventional dispersion-curve processing (Figure 1a) using the entire record in a single pass, transforming the dispersion-curve trend in the image using nineteen 3.2-s windows in 1.6-s increments appears clearer and sharper (Figure 1b).

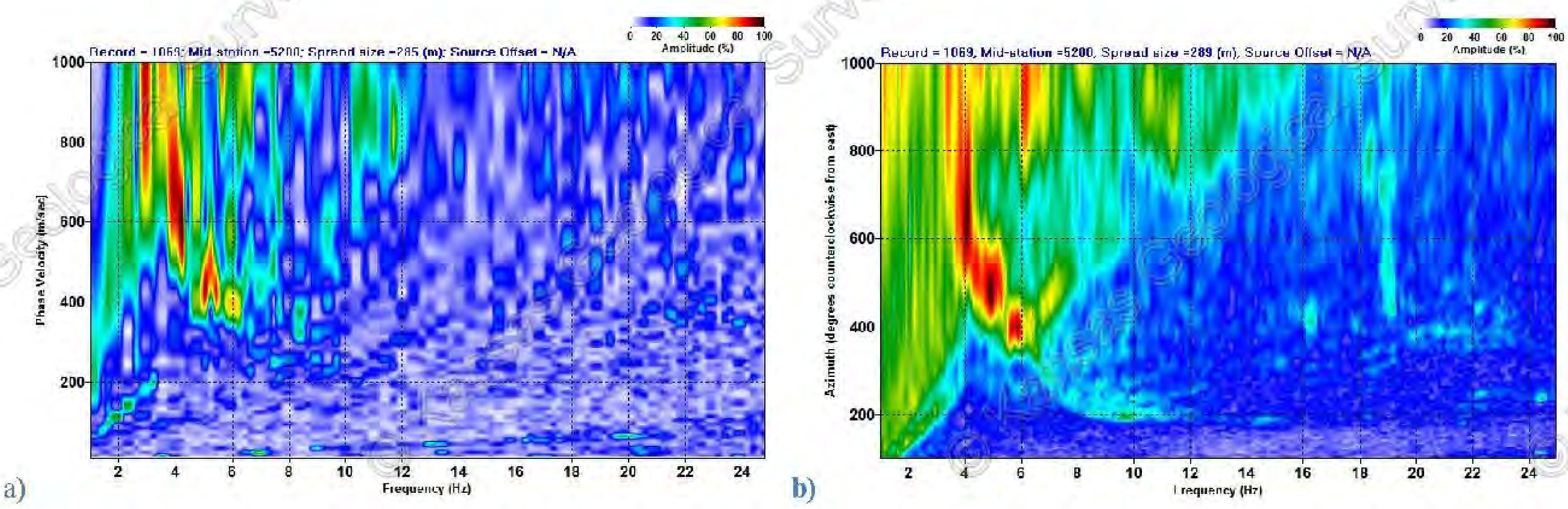

Figure 1. Conventional a), and sliding (1.6 s) window (3.2 s) b) dispersion-curve imaging.

The raw passive seismic data set, Rec(1069).dat, can be found in SurfSeis4 …\SampleData\PassiveLinear sub-folder. Sliding window analysis is activated by checking the "Enable Split" check box, at the "Records and Algorithms" tab of the "Phase-Velocity – Frequency (Overtone [OT]) Generator" dialog window (Figure 2). By default the program will select the window size to be one tenth of the total record length (e.g., 3200 ms) and the sliding scroll size to be half of that (e.g., 1600 ms).

Figure 2. "Records and Algorithms" tab of the "Phase-Velocity – Frequency (Overtone [OT]) Generator" dialog window.

We encourage the users to experiment a bit in search of the optimal window size and scrolling parameters. The algorithm stacks all the images from the windows into a single image and calculates the root-mean-square difference between the stacked image and each individual image, providing an analysis of those calculations (Figure 3a). The user can decide to use only a portion of these records with the smallest rms difference by inputting a value in the “Keep %” field (e.g., 50 instead of 100; Figure 2). The corresponding “Split Stack Message” window will provide information about which records were selected for use in the stacked image (Figure 3b).

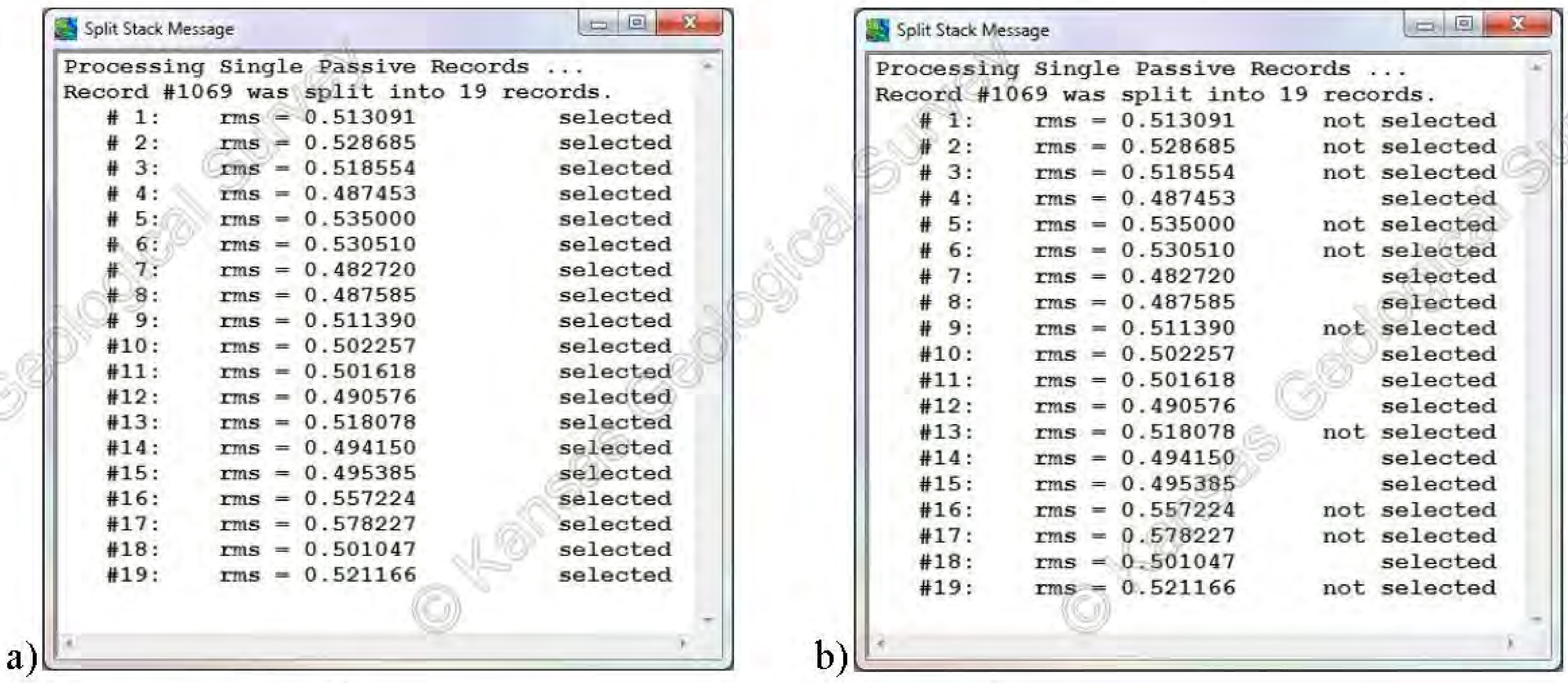

Figure 3. “Split Stack Message” window showing the rms difference between the stacked image and each individual image when all the records were used a) and when 50 % of the records were used b).

The optimal selection of what % to keep can be determined for each record (Figure 4), with that optimal selection influenced by various factors such as ambient noise, frequency and velocity ranges of the dispersion-curve image, source location (i.e., Searching Quadrants), etc.

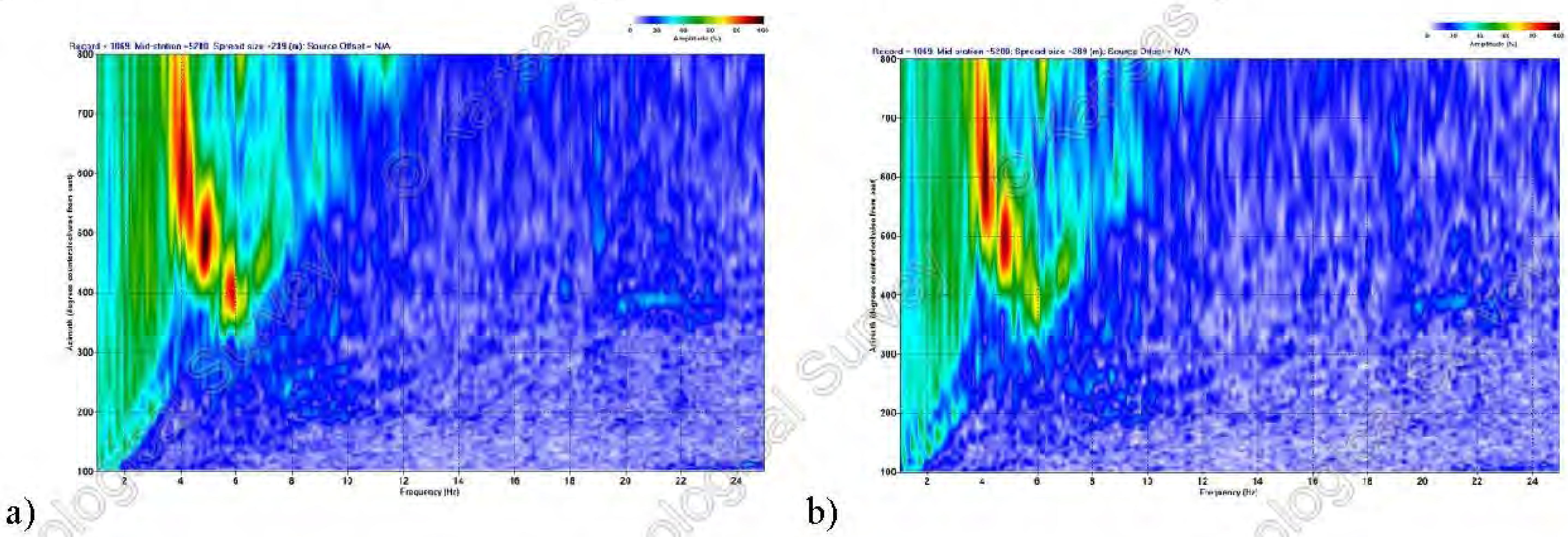

Figure 4. Sliding-window images keeping 50% a) and 25% b) of the windows with the smallest rms.

The dispersion-curve images obtained from the sample data, Rec(1069).dat, were analyzed by selecting “Inline Wave Propagation” (i.e., Offline distance = 0) and moving from the left blue arrow.

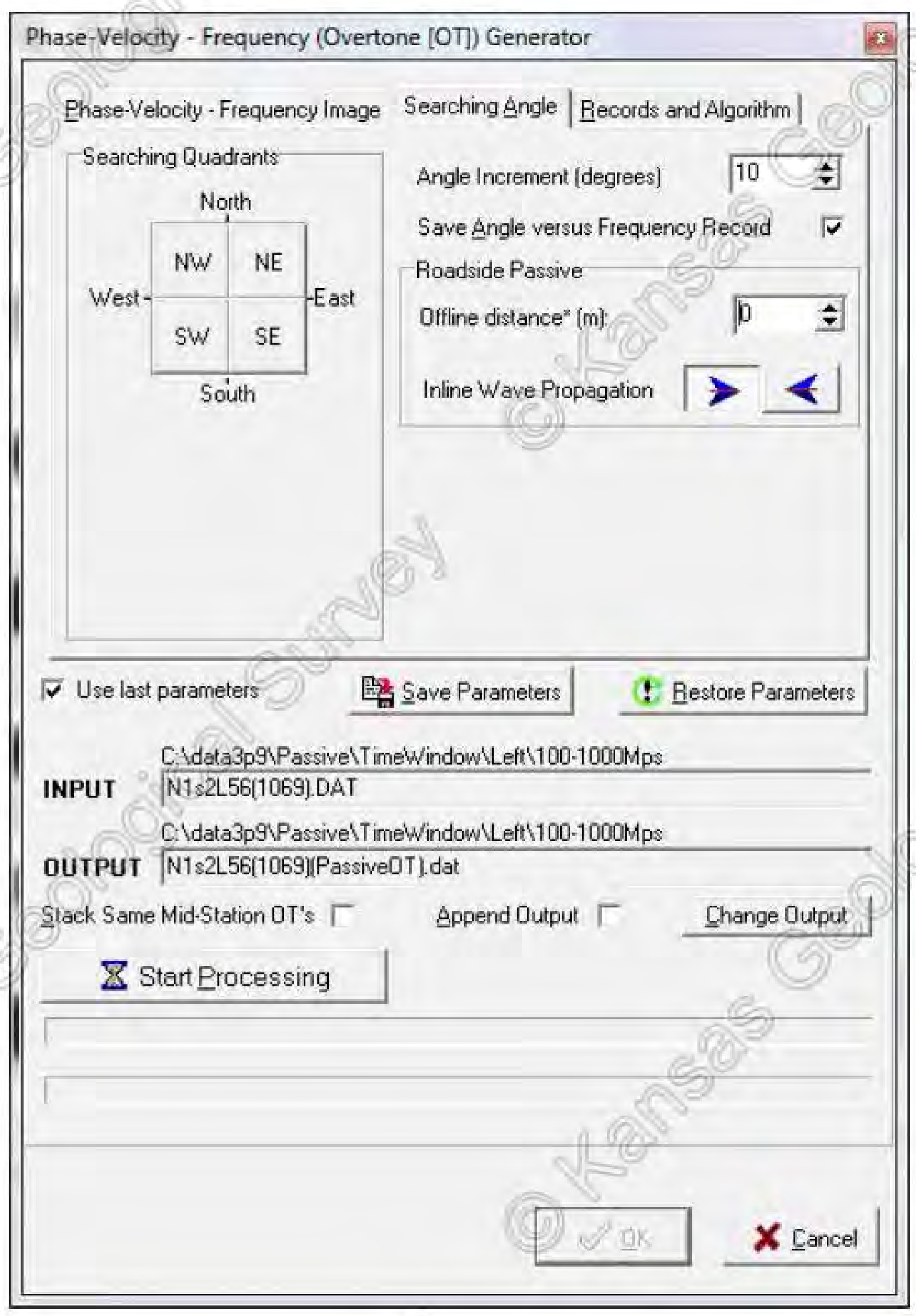

Figure 5. "Searching Angle" tab of the "Phase-Velocity – Frequency (Overtone [OT]) Generator" dialog window.

Flexible initial-model *a-priori* information input

The opportunity to provide additional initial-model a-priori information input is possible after the user starts the inversion processing (e.g., by choosing "Processing Steps", "Invert Dispersion Curves" from the menu) and opens a set of dispersion-curve files (i.e., *.dc).

The "Inversion Control" tab (formerly named "Velocities") window is displayed after the user opens the dispersion-curve files selected for inversion (e.g., 23 files) (Figure 6). In addition to the previously existing second tab ("1-D Pois and Density") there are now eight additional tabs, 4 for the initial and 4 for the final Vs, Vp, PR, and Density 2-D models, respectively.

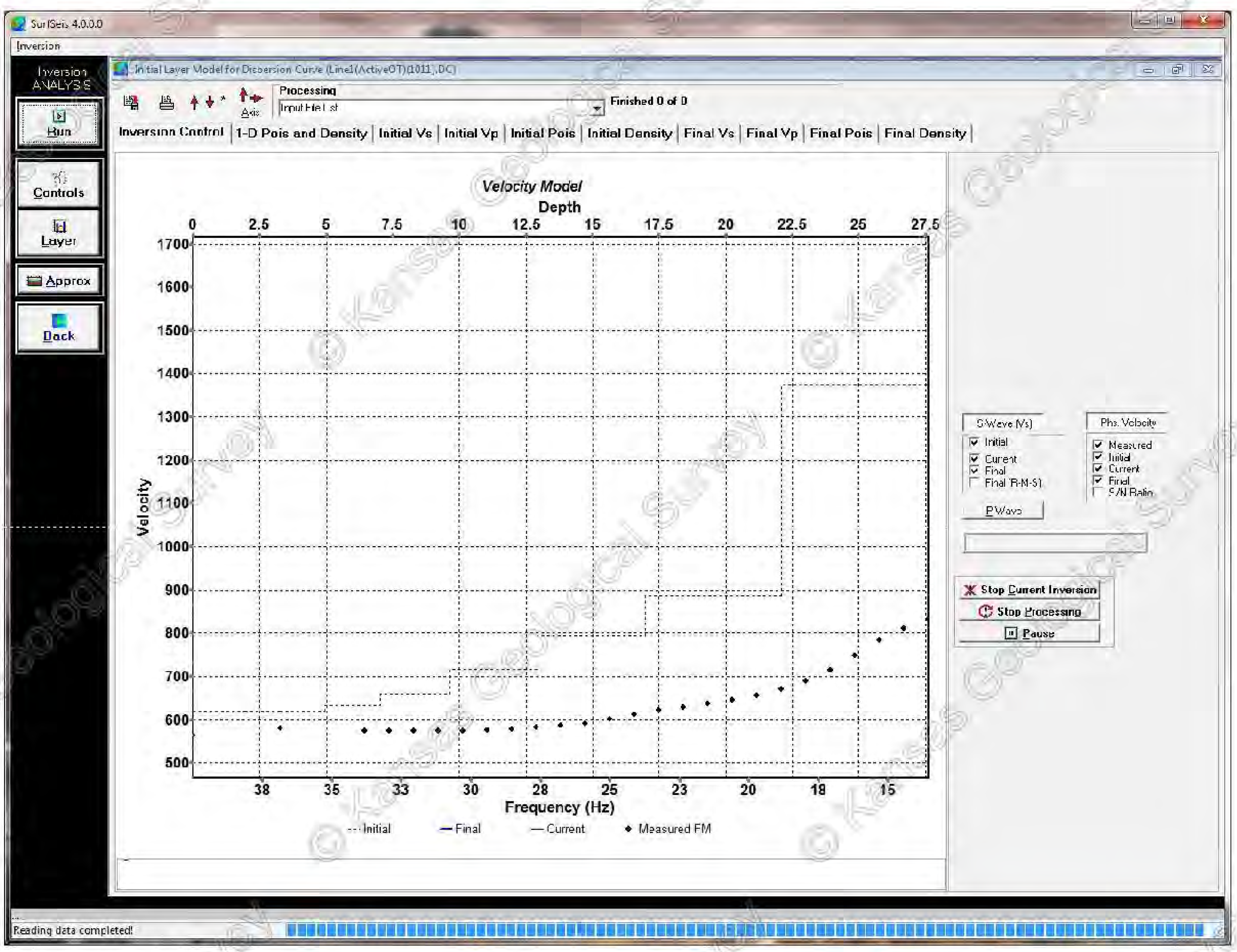

Figure 6. "Inversion Control" tab of the "Inversion" window.

Default Initial Model

The "Initial Vs" tab displays a 2-D image (Figure 7a) obtained by using an initial 1-D Vs model derived from each of the dispersion-curve files. By default, the initial PR is defined to be 0.4 for all layers and stations (Figure 7b). As a result, the calculated Vs and PR 2-D Vp model (Figure 7c) is displayed with a transparent grid overlay indicating these data are derived from default initial data (i.e., Vs and PR). The "Initial Density" tab displays a 2-D image (Figure 7d) obtained from assuming a density gradient (1.5-2) for all stations.

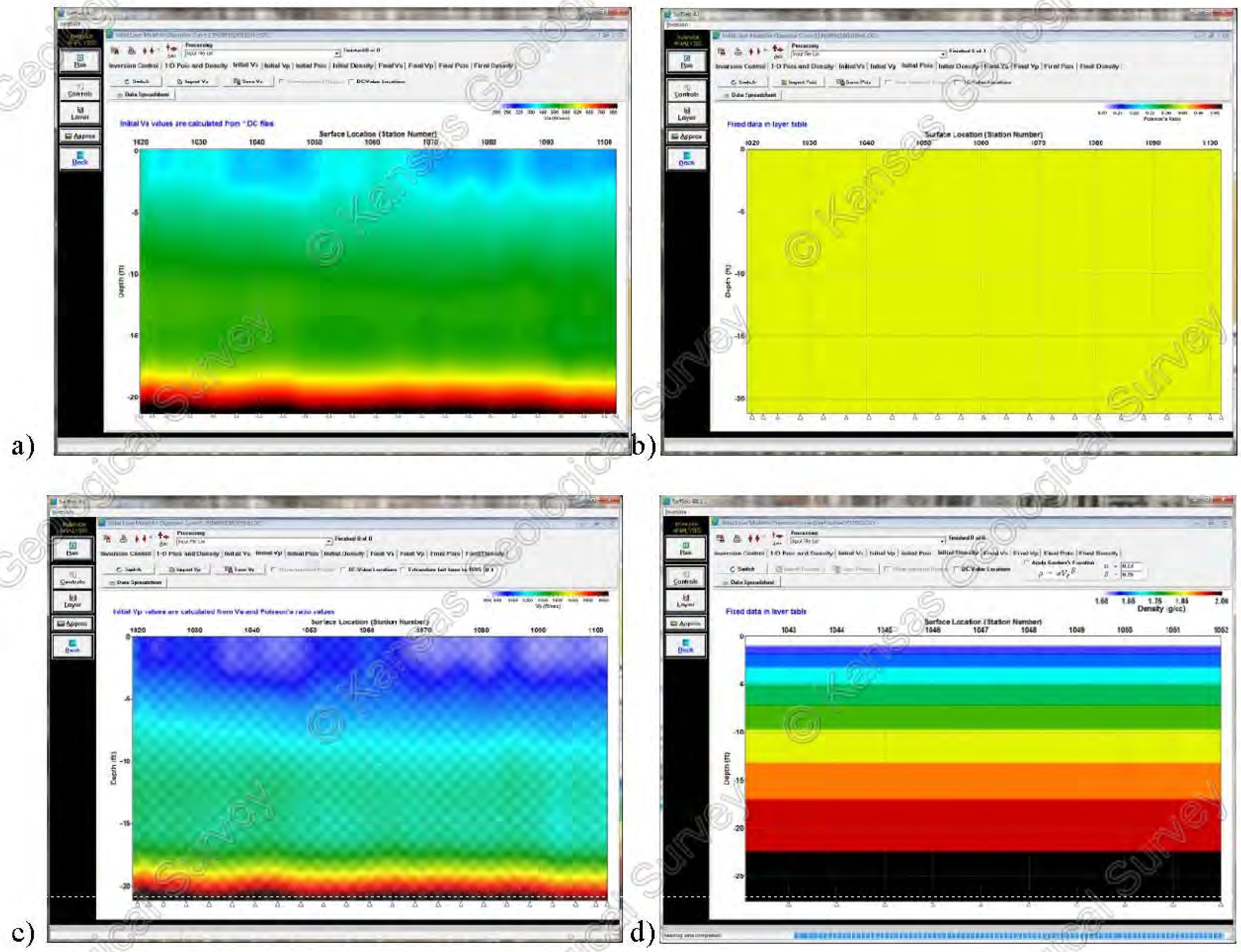

Figure 7. Initial Vs a), Poisson's ratio b), Vp c), and Density d) 2-D models.

These initial 2-D model dependencies are revealed using the "Initial Layer Model" tab (Figure 8) of the "Inversion Controls" window, which can be activated by clicking on the "Controls" button on the left side of the toolbar. These 4 Initial 2-D models can be modified in a multitude of ways.

Figure 8. "Inversion Controls" window with "Initial Layer Model" tabs active.

1-D Layer Model to 2-D

One way to change the 2-D models is by activating the "Initial Vs" tab and clicking the "Switch" button (Figure 9). The same result can be obtained by clicking on the "Fixed data in layer table" radio button (Figure 8).

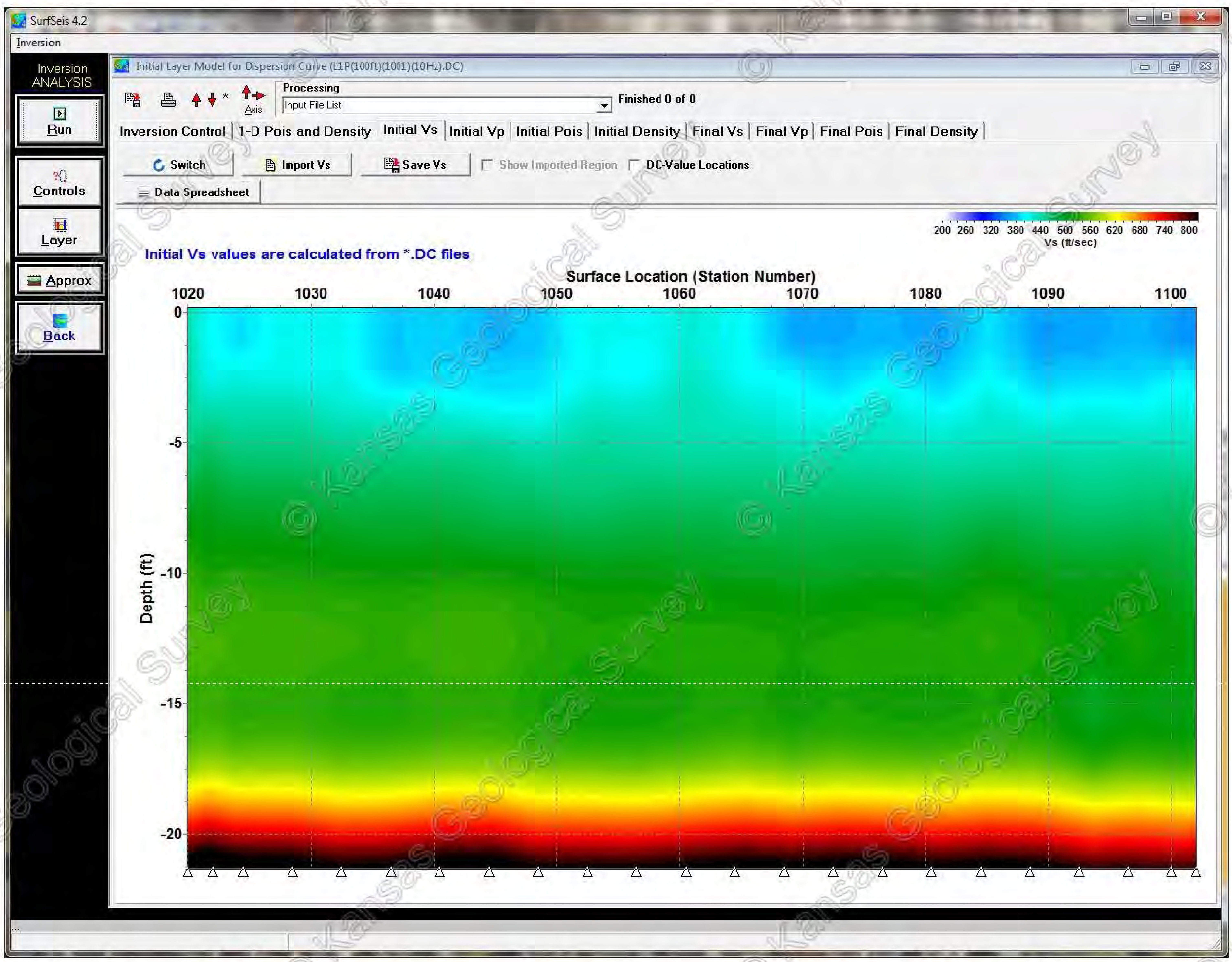

Figure 9. "Initial Vs" tab showing a 2-D Vs calculated from *.DC files.

As a result, the default 1-D layer model (estimated after considering the dispersion-curve files or imported) is expanded (Figure 10a) across the whole section. Consequently, the initial 2-D Vp model is recalculated from Vs and PR (Figure 10b). Now compare these initial model results to those in Figure 7 (a and c).

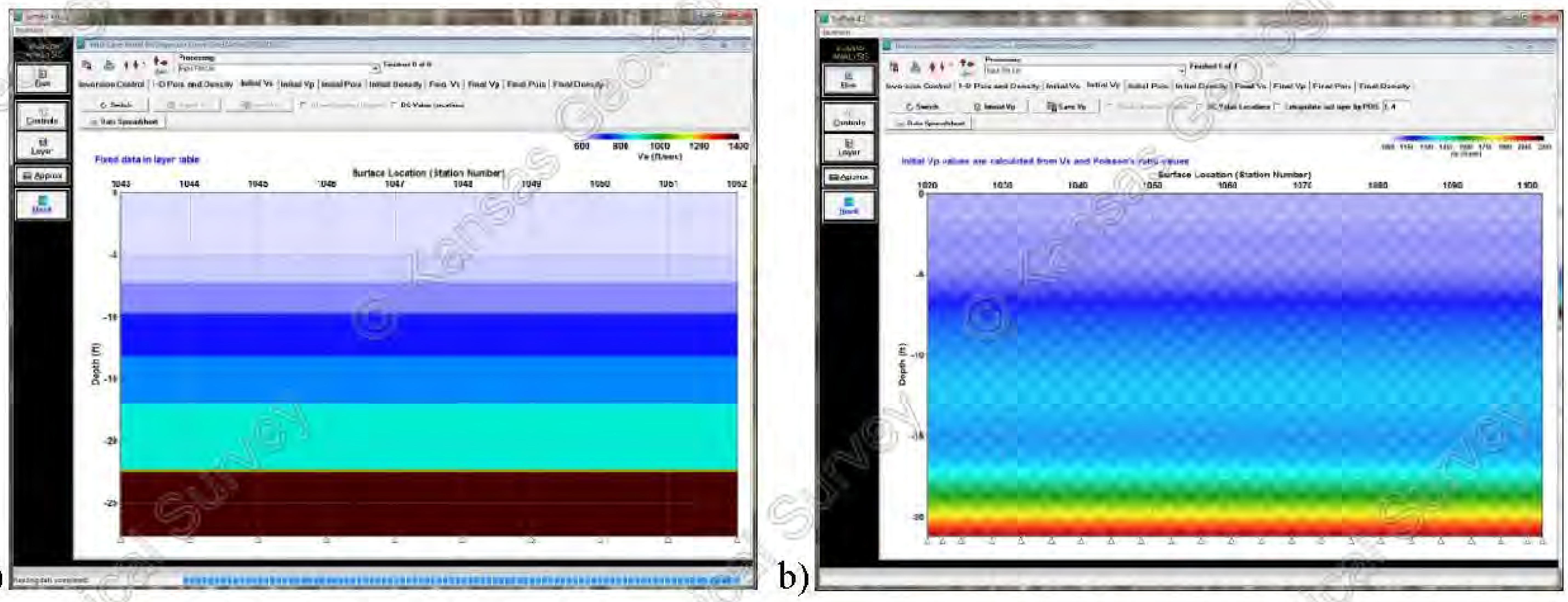

Figure 10. "Initial Vs" tab showing a 2-D Vs model calculated from 1-D layer model a) and "Initial Vp" tab showing the corresponding 2-D Vp model b).

The initial 2-D models taken directly from the 1-D layer model are displayed in stripes intentionally to tip the users about their selection (Figure 7d and Figure 10a).

The initial-model generation rule is reflected in the "Initial Layer Model" tab of the "Inversion Controls" window (Figure 11).

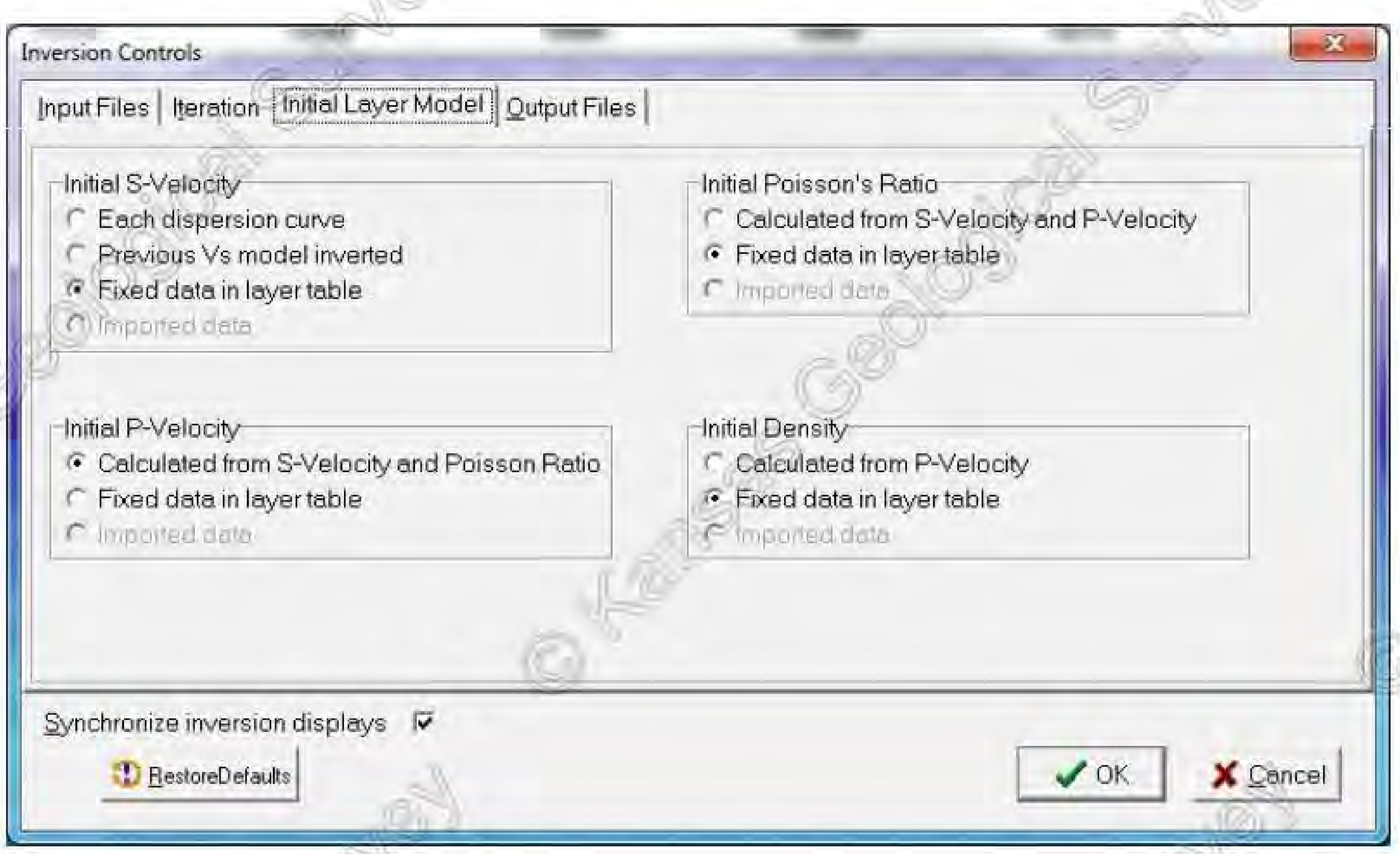

Figure 11. "Inversion Controls" window with "Initial Layer Model" tab active.

Notice in comparison that the only change between this window (Figure 11) and the previous representation (Figure 8) is the "Initial S-Velocity" radio button selecting between "Each dispersion curve" and "Fixed data in layer table." The radio buttons under the "Initial Layer Model" tab can also be used to change the resulting initial models. However, the discussion in this document will continue using the 2-D images for convenience.

Repeated clicking of the "Switch" button on the "Initial Vs" tab will continue changing back and forth between the two 2-D Vs models (Figure 7a and Figure 10a) with the initial 2-D Vp model changing accordingly.

Import 2-D Models

Another way of introducing initial model data is through the "Import …" button, which can be found next to the "Switch" button on each of the "Initial …" tabs. Clicking on "Import Vp" and selecting a file name (.grd or .txt format) imports Vp data (Figure 12a) estimated by other methods, such as borehole data and refraction tomography. Under this scenario the Vp data takes the lead (greatest weighting) in calculating PR (Figure 12b).

a) 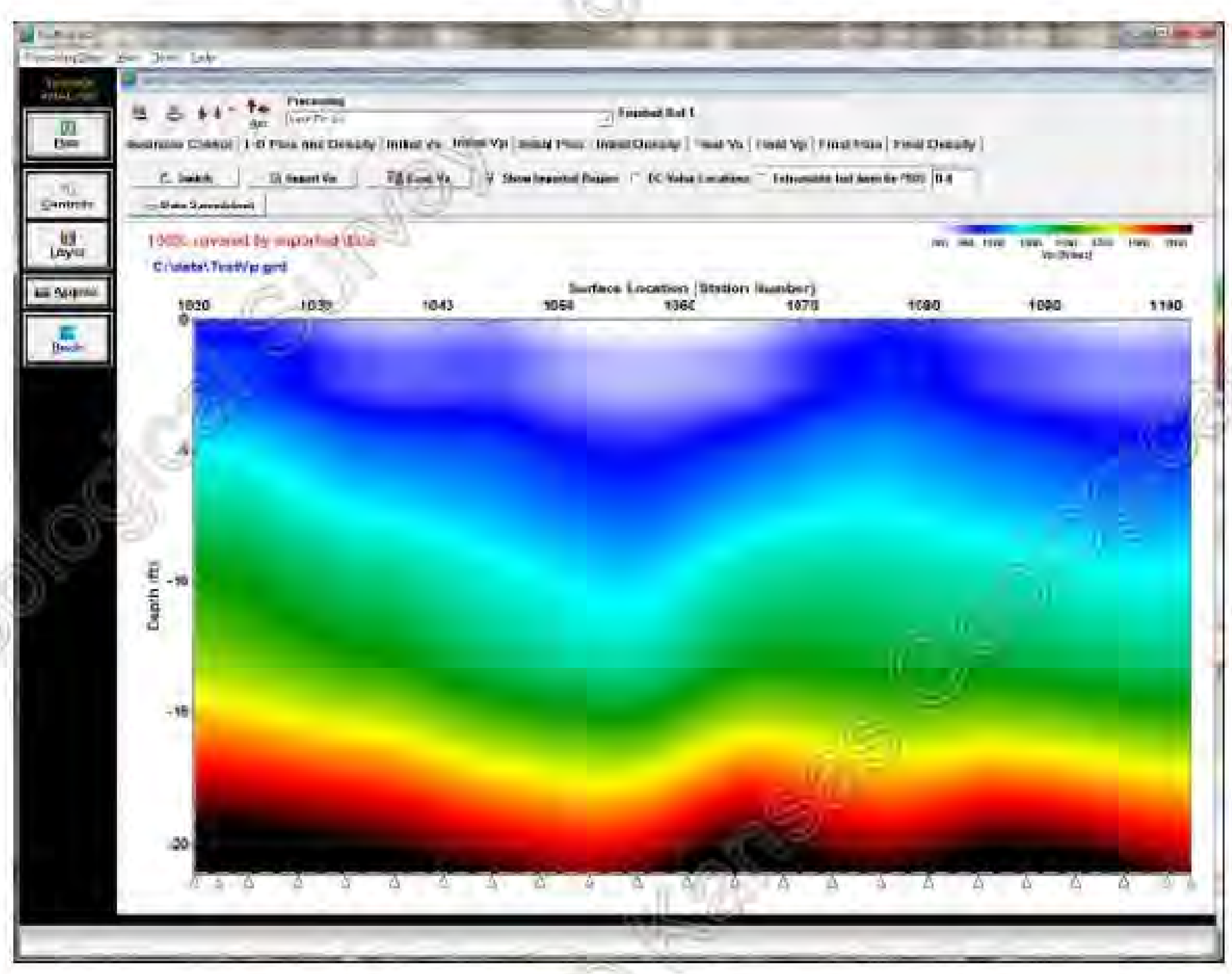 b) 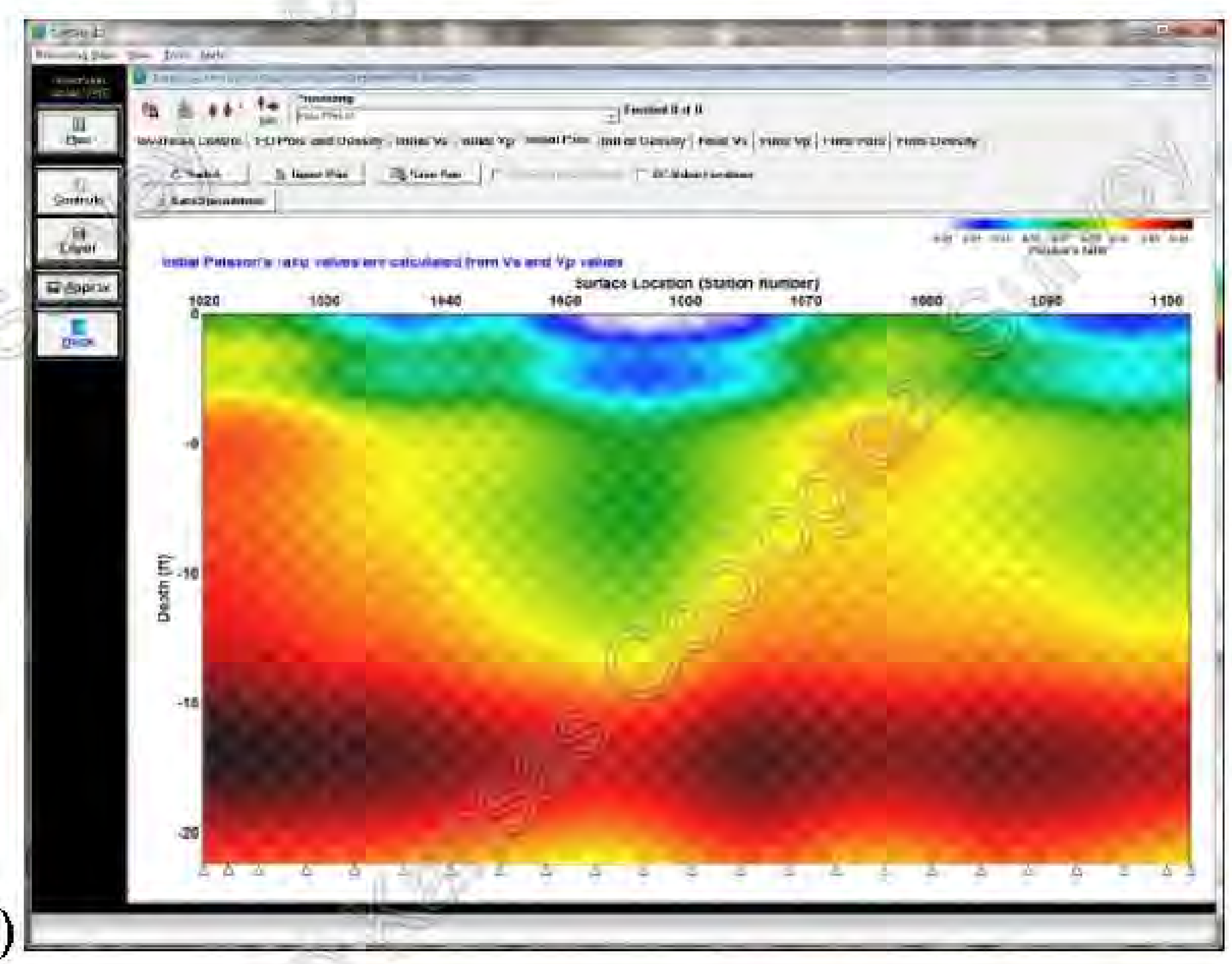

Figure 12. "Initial Vp" tab showing an imported 2-D Vp model a) and "Initial Pois" tab showing the resulting 2-D PR model b).

Import-data formats can be text (i.e., ASCII) *.grd, 3-column *.txt, and layer-model *.lyr files. The 3-column *.txt file will be automatically converted to *.grd format and the *.lyr file will be used to import only the value under consideration (e.g., PR).

Again, the initial 2-D model controls are reflected in the "Initial Layer Model" tab (e.g., Figure 8 and Figure 11) of the "Inversion Controls" window. Poisson's ration, Vs, and Vp are mutually dependent. Any one of them can be calculated from the other two.

For imported data that does not include the full range of Vs initial values, missing data points are populated by extrapolating from the nearest values (Figure 13a). The image can be somewhat different than expected because it reflects the fact that actual values are assigned to relatively thick layers used to make the displayed image. To better match this displayed image with expectations, it is possible to change the Vp values of the last layer (a.k.a., half space) using the "Extrapolate last layer by POS" button, which has a default value of 0.4 (Figure 13b).

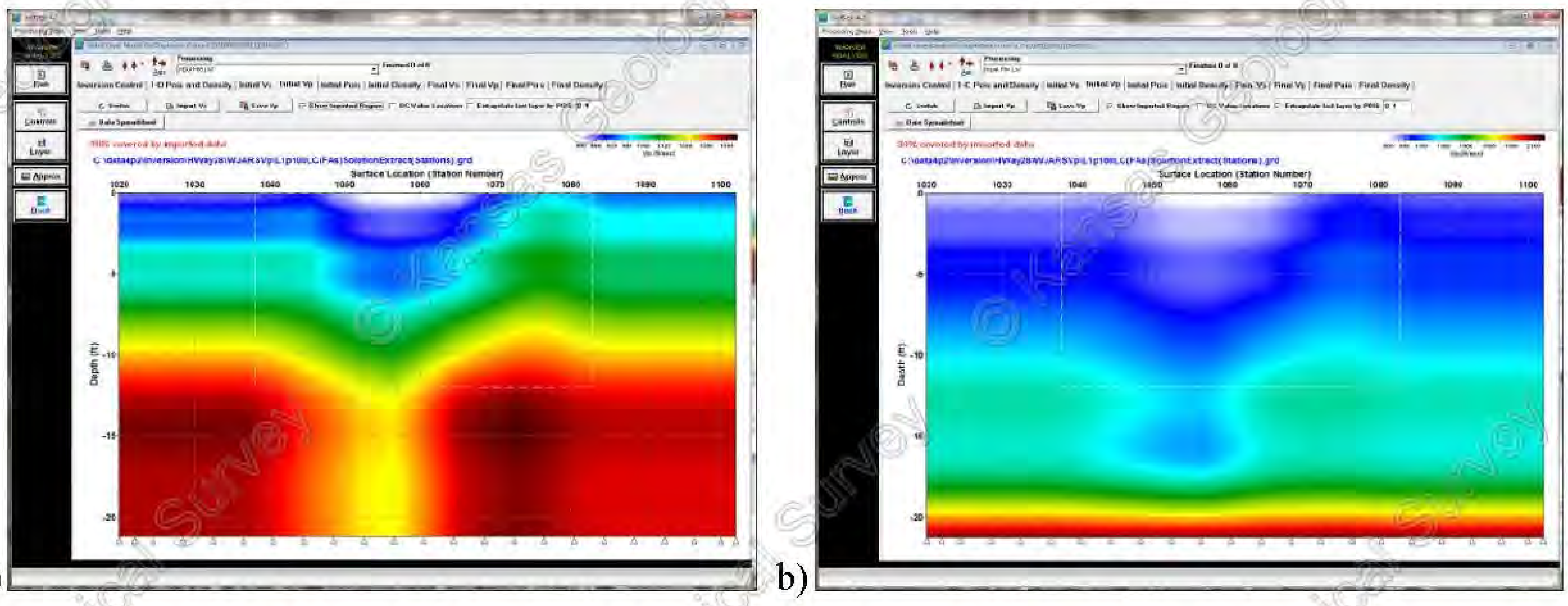

a) b)

Figure 13. "Initial Vp" tab showing an imported 2-D Vp model that is smaller than needed (marked with a white dashed rectangle) a) and extrapolating last layer by Poisson's ratio of 0.4 b).

Other 2-D Model Considerations

Density derived using Gardner's equation

In addition to using the layer model table or importing 2-D data from another file, density can be calculated from Vp using Gardner's equation and default coefficients. Additionally, users can chose other coefficients.

2-D Model from 1-D layer

As usual, the 1-D layer model can be modified using the "Layer" button and the table upgraded through the "Layer Parameters" window (Figure 14). The layer model can be saved into or imported from a *.lyr file.

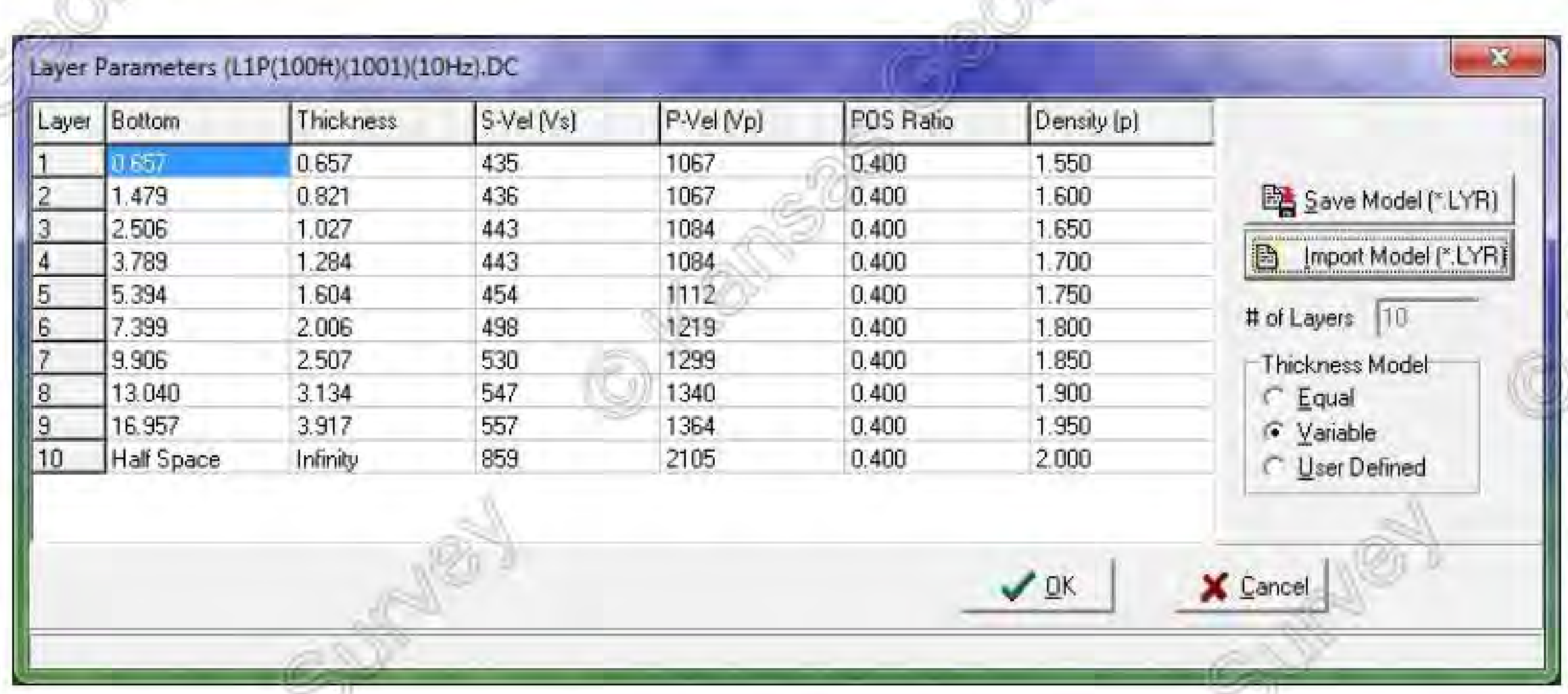

Layer Parameters (L1P(100ft)(1001)(10Hz).DC

Layer	Bottom	Thickness	S-Vel (Vs)	P-Vel (Vp)	POS Ratio	Density (p)
1	0.657	0.657	435	1067	0.400	1.550
2	1.479	0.821	436	1067	0.400	1.600
3	2.506	1.027	443	1084	0.400	1.650
4	3.789	1.284	443	1084	0.400	1.700
5	5.394	1.604	454	1112	0.400	1.750
6	7.399	2.006	498	1219	0.400	1.800
7	9.906	2.507	530	1299	0.400	1.850
8	13.040	3.134	547	1340	0.400	1.900
9	16.957	3.917	557	1364	0.400	1.950
10	Half Space	Infinity	859	2105	0.400	2.000

Figure 14. Layer model table.

The 1-D layer model values displayed by the "Layer Parameters" are the same ones used for the 2-D Vs model calculated from 1-D layer model in Figure 10a.

Initial model spreadsheets

The actual data values estimated from the imported data and used in the layer-based model inversion can be viewed by clicking the "Data Spreadsheet" button (Figure 13b) and edited by typing new data values in individual cells (Figure 15a). The corresponding 2-D data image will be renewed (Figure 15b) after clicking the "Update" button on the spreadsheet. Then the data can be saved as a text .grd file for future use and reference. The saved grid will be consistent with the imported grid, which might be different than the spreadsheet table representing stations and layers used in the inversion.

a) 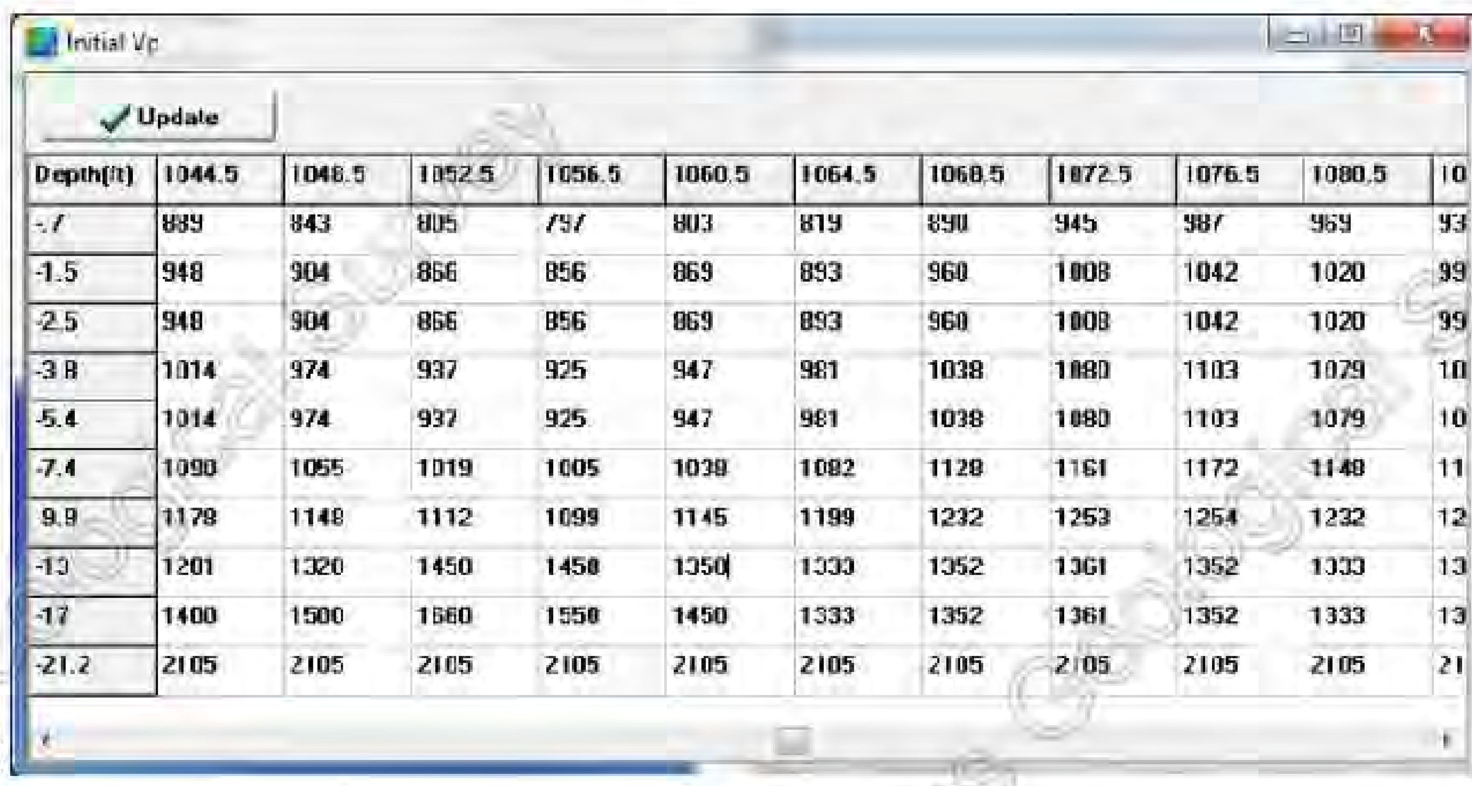

Initial Vp

Update

Depth(ft)	1044.5	1048.5	1052.5	1056.5	1060.5	1064.5	1068.5	1072.5	1076.5	1080.5	10
-.7	889	843	805	797	803	819	890	945	987	969	93
-1.5	948	904	866	856	869	893	960	1008	1042	1020	99
-2.5	948	904	866	856	869	893	960	1008	1042	1020	99
-3.8	1014	974	937	925	947	981	1038	1080	1103	1079	10
-5.4	1014	974	937	925	947	981	1038	1080	1103	1079	10
-7.4	1090	1055	1019	1005	1038	1082	1128	1161	1172	1148	11
9.9	1178	1148	1112	1099	1145	1199	1232	1253	1254	1232	12
-13	1201	1320	1450	1458	1350	1333	1352	1361	1352	1333	13
-17	1400	1500	1560	1550	1450	1333	1352	1361	1352	1333	13
-21.2	2105	2105	2105	2105	2105	2105	2105	2105	2105	2105	21

b) 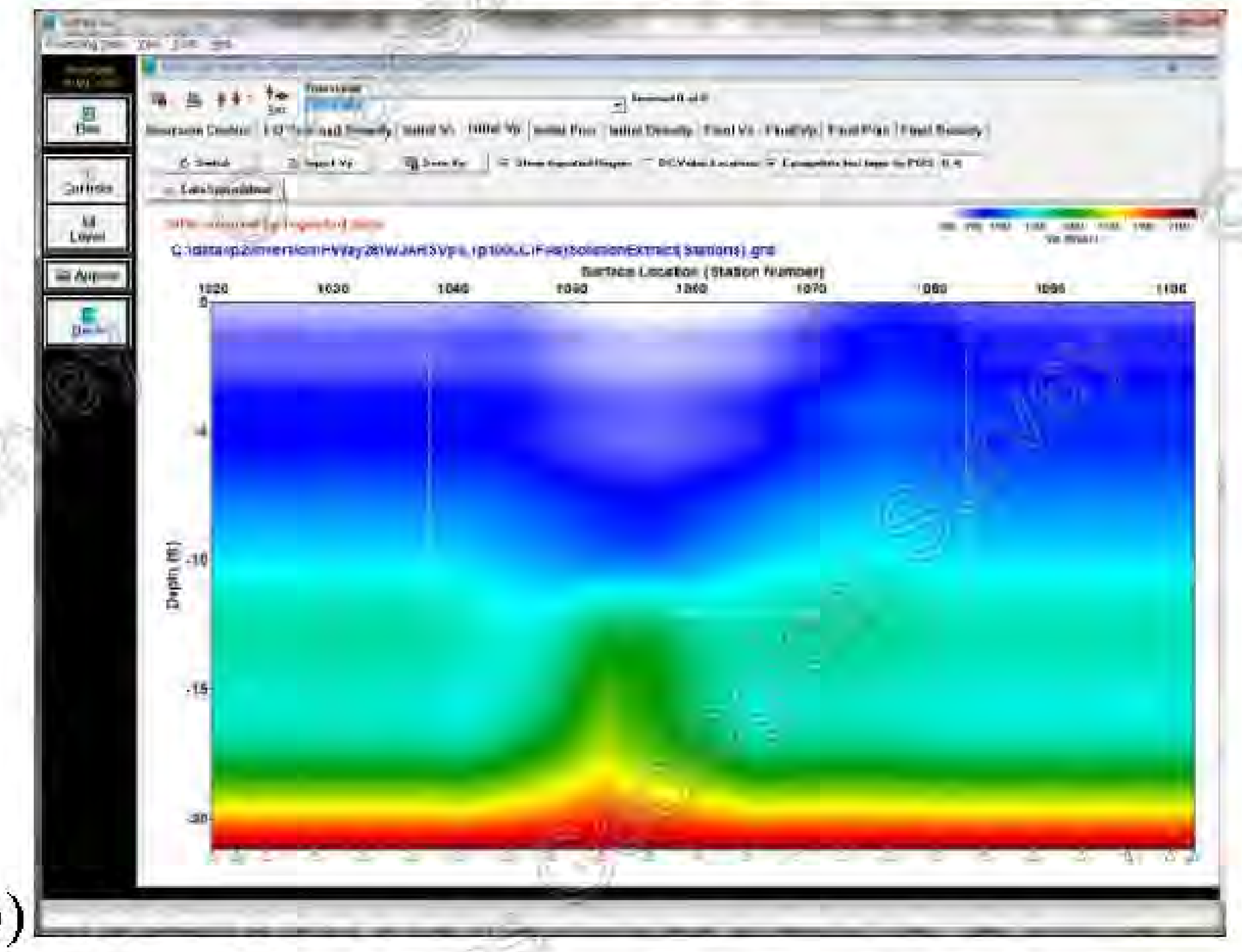

Figure 15. Layer-based Spreadsheet that can be edited a), with a corresponding 2-D image renewed after clicking the "Update" button b).

Data in all these examples were used to demonstrate different relatively common software possibilities and are not intended to be considered ideal for all types of estimations or interpretations.

Ongoing-inversion 2-D images of *Vs*, *Vp*, *PR*, and *Density*

In addition to the current dispersion-curve inversion at the "Inversion Control" tab observed after the user clicks the "Run" button, it is possible to display the 2-D Vs model at the "Final Vs" tab as it updates after each dispersion-curve 1-D Vs inversion. This provides an excellent way to view the forming 2-D image as it develops (Figure 16).

Similarly, there are "Final Vp", "Final Pois", and "Final Density" tabs where the user can follow the development of the inversion 2-D images of specific parameters. Vp or PR 2-D image (at "Final Vp"or "Final Pois" tab) will change from the initial model based on the choice of parameter to keep fixed during the inversion. 2-D Density images will not change but is provided here for convenience. Still, these Vp, PR, and Density data need to be considered only as *a-priori* information used for the surface wave inversion and should not be treated as analysis output results. Such results can be obtained with higher accuracy other geophysical methods.

There is also a movable mini-inversion-control window showing the inversion process of the current dispersion curve and allows the user to stop current iteration, the inversion processing, or simply pause the process (Figure 16).

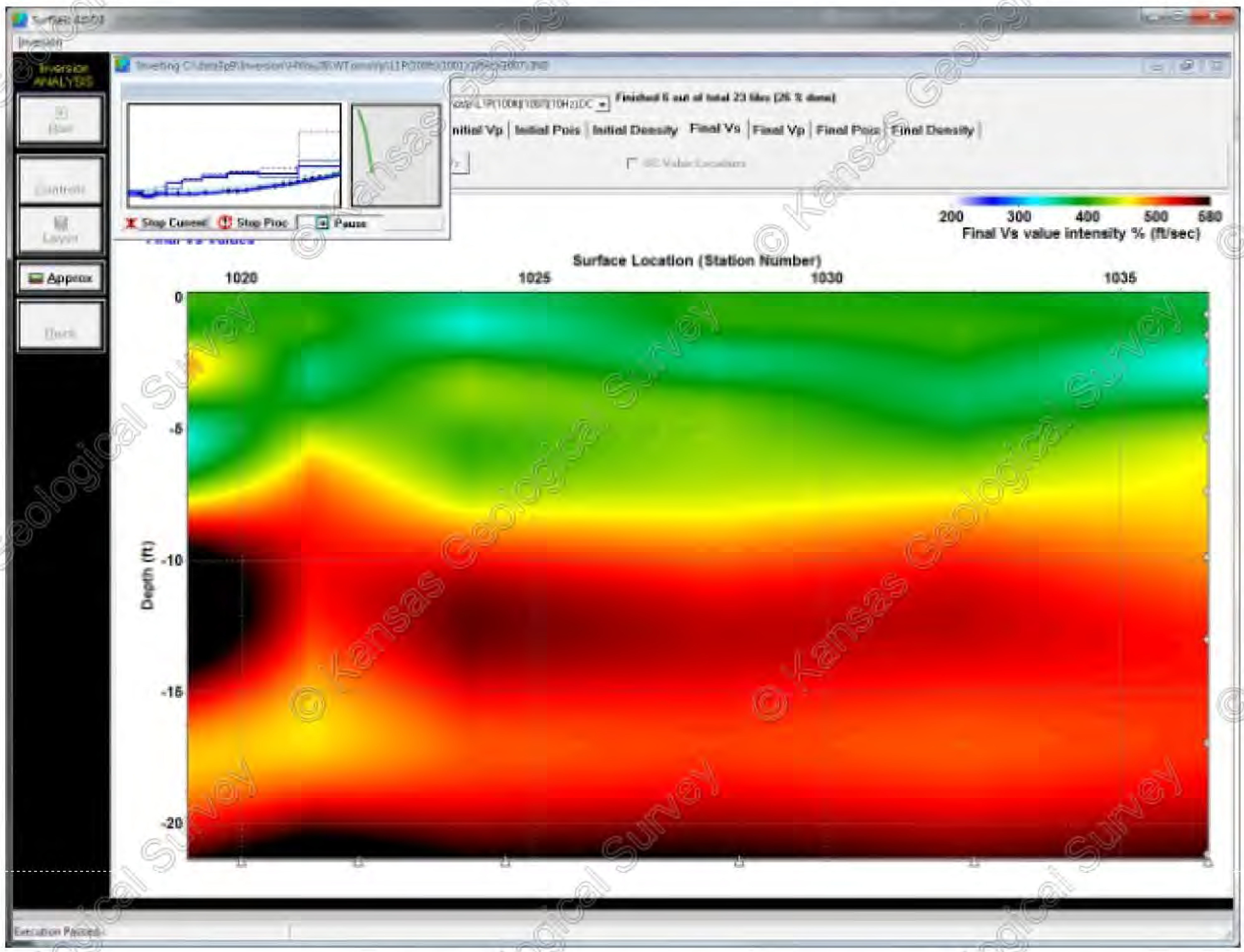

Figure 16. "Final Vs" tab showing an ongoing 2-D Vs image calculated from just-inverted 6 (during the inversion of 23) dispersion curves. White triangles at the bottom of the image show the horizontal location of the corresponding 1-D Vs sections. Mini-inversion-control window can be noticed in the upper right corner of the image.

New output possibilities

Center-of-the-layer 3-column output

Traditionally, SurfSeis uses bottom-of-the-layer depths format to preserve and provide information about layer thicknesses and depths, including in the output .lst and .txt files. However, when using the inversion result for 2-D gridding (i.e., interpolation) and imaging it is more appropriate to use center-of-the-layer depths. For this purpose a new set of 3-column text file is offered with a "(c)" appended to the root output file name, which can be activated using a "Use layer-centered output" checkbox (Figure 17).

Inversion-files naming derived from root output-file name

The inversion related files names (e.g., *.LST) are now derived from the root of the output file name (Figure 17) instead of the input *.DC file name. This allows for a set of dispersion curves to have more than one inversion session run in the same folder using different inversion parameters, while preserving the information from each inversion. The root output file name can be changed using the "Change File Name…" button.

Default Vp output

As usual, Vp values used during the inversion are saved in the *.LST file. For users convenience the information from all *.LST files is now saved by default into a 3-column text file that will have "(Vp)" appended to the root output file name. Again, Vp values should not be considered as output results from surface-wave analysis but only values used diring the inversion. They can be identical to the initial Vp model or be calculated from the initial Poisson's ratio model and Vs inversion results (when Poisson's ratio the is chosen to be fixed during the inversion).

Poisson's ratio and Vp/Vs ratio output

Poisson's ratio and Vp/Vs ratio values can be calculated from the output results and saved as 3-column text files (*.TXT) for convenience, if users check the "Output Poisson's Ratio and Vp/Vs Ratio" checkbox. The corresponding file names will have "(Pois)" and "(VpVsRatio)" appended to the root output file name accordingly.

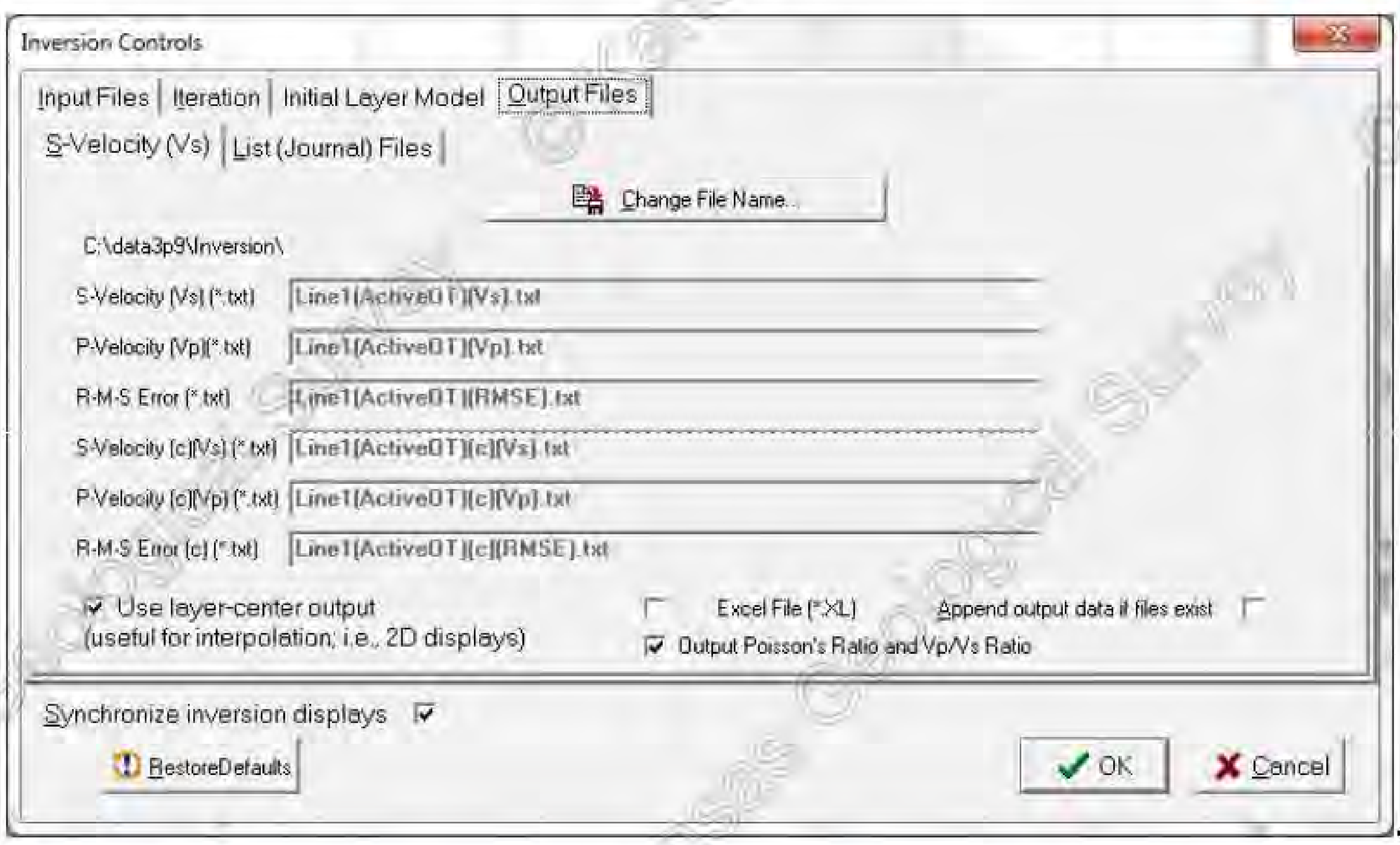

Figure 17. "Inversion Controls" window with "Output Files" tab active.

High-Resolution Linear Radon Transform (HRLRT) for dispersion-curve imaging (optional, included in SurfSeis 4.2)

Dispersion-curve imaging using the HRLRT is included in SurfSeis 4.2 version. It is software developed based on the work by Luo, et al. (2008) and is preferred by many researchers (Zeng, et al., 2012; Pan, et al., 2013) over standard methods of dispersion-curve imaging. It can be helpful for separating and interpreting different surface-wave modes (Ivanov, et al., 2010), especially when the rest of the d-c imaging methods (Park et al., 1998; Xia et al., 2007) are not able to separate them and as a result display merged trends.

We use the 2-layer velocity model (Figure 18a) to generate 60-trace synthetic seismic data similar to that used in previous research (Xu et al., 2007; Luo, et al., 2008) (Figure 18b). A 25 Hz first derivative Gaussian wavelet and KGS's Rayleigh-wave-tuned synthetic seismic data modeling software (scheduled for future release) based on the research by Zeng et al. (2011) are

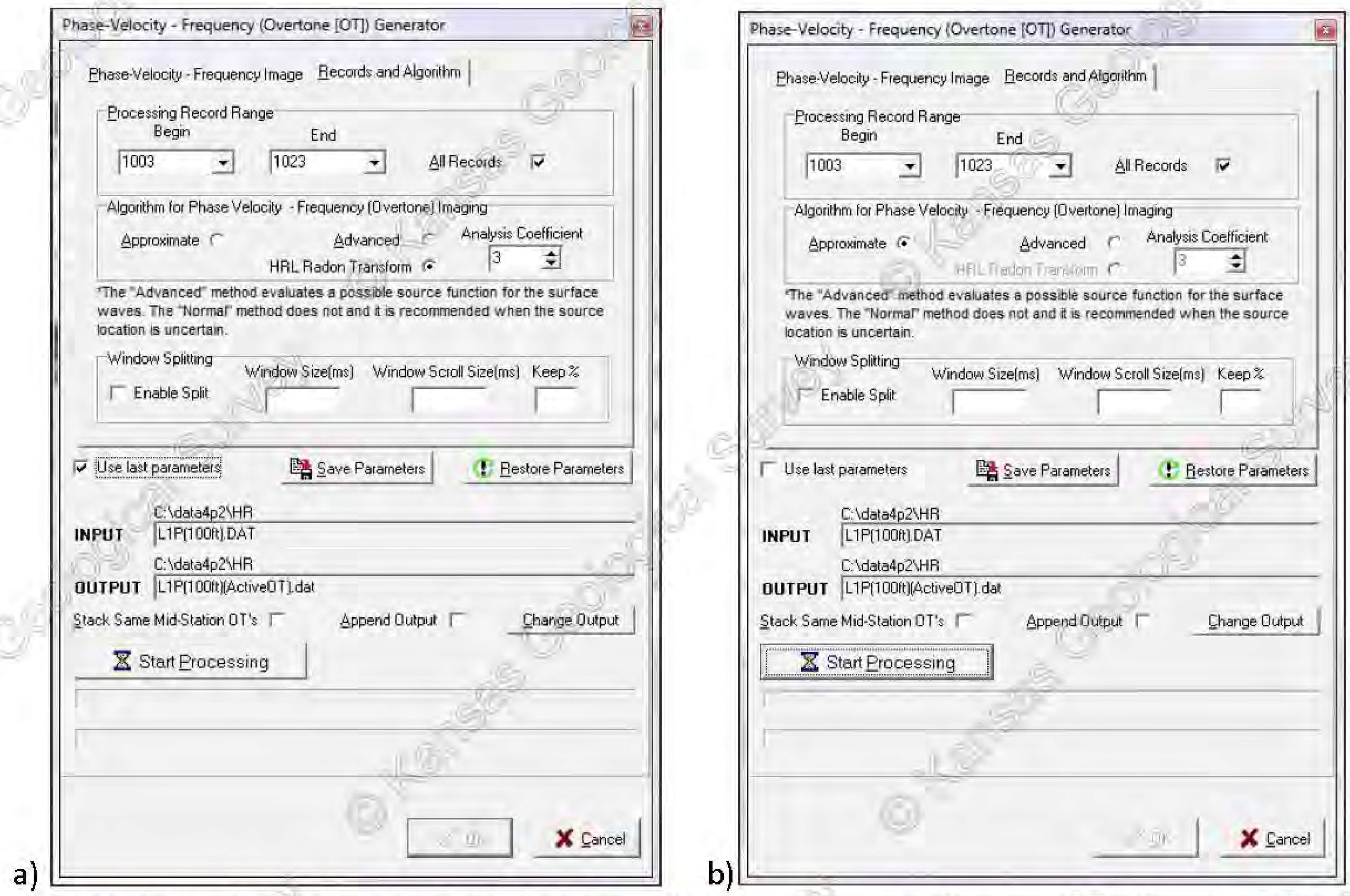

Figure 20. **"Records and Algorithms" tab of the "Phase-Velocity – Frequency (Overtone [OT]) Generator" dialog window with the "HRL Radon Transform" selected.**

USB Dongle Administration

Upgrading from SurfSeis 3 versions

If you are upgrading from SurfSeis 3 to either SurfSeis 4.0 or SurfSeis 4.2, you will need to update the dongle you have been using with SurfSeis 3 so you can use the new software features. Updating the dongle is accomplished by applying a V2C (Vendor-to-Customer) file to your dongle. In many instances the SurfSeis software administrator (Mary Brohammer at the Kansas Geological Survey) will be able to generate this file because she has the database that contains information specific to your dongle. In some instances you may be asked to generate a C2V file and submit it before the upgrade to your dongle can be processed. For more information see Manual3.05.pdf from your SurfSeis 3 installation (e.g., in C:\SurfSeis30\Manual folder) or visit KGS's web site for SurfSeis.

Licensing compatible with Windows 8

We use third-party software, SafeNet Sentinel HASP, for our software licensing protection. We use their most recent version, LDK 7.0, which they indicate is compatible with Windows 8.

Our experience with Windows 8 shows that sometimes after installation of SurfSeis initially the dongle is not recognized and software does not run. Uninstalling and installing the Sentinel HASP driver may fix the problem and the software will function. In some occasions after uninstalling the driver Windows 8 may automatically install it and the SurfSeis will run.

Sometimes it might be necessary to uninstall the driver (e.g., when you are doing a Windows 8 upgrade).

We provide Sentinel HASP (version 6.60, part of LDK 7.0) driver in the "HaspDriver" SurfSeis4 sub-folder with instructions (i.e., .docx, .txt, and .html files) and "InstallHaspDriver.bat" and "UninstallHaspDriver.bat" files your for convenience. Check if there is a newer driver available at SafeNet's web site (a.k.a., www.aladdin.com/hs) and click on the "Sentinel HASP/LDK - Command Line Run-time Installer" link.

Acknowledgements

We appreciate Tyler Schwenk's beta version testing and suggestions, which helped improve the final version of SurfSeis 4. We are also thankful to Mary Brohammer for the preparation of this manuscript.

References

Ivanov, J., B. Leitner, W. T. Shefchik, T. J. Schwenk, and S. L. Peterie, 2013, Evaluating hazards at salt cavern sites using multichannel analysis of surface waves: The Leading Edge, **32**, 289-305.

Ivanov, J., R. D. Miller, J. Xia, and S. Peterie, 2010, Multi-mode inversion of multi-channel analysis of surface waves (MASW) dispersion curves and high-resolution linear radon transform (HRLRT): 80th Annual International Meeting, SEG, Technical Program Expanded Abstracts, **29**, 1902-1907.

Luo, Y. H., J. H. Xia, R. D. Miller, Y. X. Xu, J. P. Liu, and Q. S. Liu, 2008, Rayleigh-wave dispersive energy imaging using a high-resolution linear Radon transform: Pure and Applied Geophysics, **165**, 903-922.

Pan, Y. D., J. H. Xia, and C. Zeng, 2013, Verification of correctness of using real part of complex root as Rayleigh-wave phase velocity with synthetic data: Journal of Applied Geophysics, **88**, 94-100.

Park, C. B., R. D. Miller, and J. Xia, 1998, Imaging dispersion curves of surface waves on multi-channel record 68th Annual International Meeting, SEG, Expanded Abstracts, 1377-1380.

Xia, J. H., Y. X. Xu, and R. D. Miller, 2007, Generating an image of dispersive energy by frequency decomposition and slant stacking: Pure and Applied Geophysics, **164**, 941-956.

Xu, Y. X., J. H. Xia, and R. D. Miller, 2007, Numerical investigation of implementation of air-earth boundary by acoustic-elastic boundary approach: Geophysics, **72**, Sm147-Sm153.

Zeng, C., J. H. Xia, R. D. Miller, and G. P. Tsoflias, 2011, Application of the multiaxial perfectly matched layer (M-PML) to near-surface seismic modeling with Rayleigh waves: Geophysics, **76**, T43-T52.

Zeng, C., J. H. Xia, R. D. Miller, G. P. Tsoflias, and Z. J. Wang, 2012, Numerical investigation of MASW applications in presence of surface topography: Journal of Applied Geophysics, **84**, 52-60.